On the Weibull Autocorrelation and Power Spectrum Functions: Field Trials and Validation

Ugo S. Dias, Michel D. Yacoub, Gustavo Fraidenraich, José C. S. Santos Filho, and Daniel B. da Costa

***Resumo*— Medidas de campo *indoor* e *outdoor* são utilizadas para validar a função de autocorrelação derivada de maneira exata para o desvanecimento de Weibull. Além disso, uma aproximação precisa e fechada para o espectro de potência da envoltória de Weibull é obtida e também validada. Comparações são realizadas e uma excelente concordância às medidas de campo é encontrada.**

***Palavras-Chave*— Medidas de campo, espectro de potência, função de autocorrelação de Weibull, distribuição de Weibull, validação.**

***Abstract*— Indoor and outdoor field trial measurements are used to validate the autocorrelation function derived in an exact manner for the Weibull fading signal. In addition, an *accurate closed-form* approximation to the power spectrum of the Weibull envelope is obtained and also validated. Comparisons are performed and an *excellent* fitting to the field measurements is found.**

***Keywords*— Field trials, power spectrum, Weibull autocorrelation function, Weibull distribution, validation.**

I. Introduction

The performance of the wireless channel is strongly affected by the multipath fading phenomena. In order to mitigate this effect, a deep knowledge of the characteristics and correct modeling of fading channels is imperative. Many statistical models have been used to describe the multipath fading phenomenon [1]. Some of these models produce very accurate results, especially Rice and Nakagami-m [2]. Another useful model is Weibull, which was first used in problems dealing with reliability. Indeed, the Weibull distribution is a simple and flexible statistical model for describing multipath fading phenomena, for both indoor and outdoor propagation environments.

Experimental data supporting the Weibull fading model have been reported in [3]. Indoor and outdoor applications of the Weibull model were considered in [4] and [5], respectively. In [6], the Weibull and Nakagami-*m* models were recommended for theoretical studies since it introduces slope changes in the distribution tail, which compensates for shortcomings of the Rayleigh model. In [7], measurements revealed that the Weibull distribution had the best fit to path-loss models of the narrow-band digital enhanced cordless telecommunications (DECT) system at reference frequency 1.89 GHz.

A substantial portion of the literature dealing with field measurements in Weibull fading channels has been devoted to the study of the first order statistics. Few works investigate the higher order statistics of the Weibull channel model. In [8], the level crossing rate (LCR) and the average fade duration (AFD) of the Weibull channel have been obtained, whereas in [9] these statistics have been attained for the diversity-combined case. Very recently [10], a simple closed-form expression for the generalized cross-moments of the Weibull distribution has been derived. From this expression, the derivation of the autocorrelation function follows directly.

In this paper, the autocorrelation function derived in [10] is validated through field measurements. In addition, an *accurate closed-form* approximation to the power spectrum of the Weibull envelope is also obtained and validated.

The authors are with the Wireless Technology Laboratory (WissTek), Department of Communications, School of Electrical and Computation Engineering, State University of Campinas, DECOM/FEEC/UNICAMP, PO Box 6101, 13083-852, Campinas, SP, Brazil, E-mails: [ugo,michel,gf,candido,daniel]@wisstek.org. This work was supported in part by CAPES.

II. The Autocorrelation Function

The temporal autocorrelation function $A_R(\tau)$ of the Weibull envelope R has been recently obtained in [10] as

$$A_R(\tau) \triangleq E[R(t)R(t+\tau)] = \hat{r}^2\,\Gamma^2\left(1+\frac{1}{\alpha}\right)\,{}_2F_1\left(-\frac{1}{\alpha},-\frac{1}{\alpha};1;J_0^2(\omega_D\tau)\right) \quad (1)$$

where $\hat{r} = \sqrt[\alpha]{E[R^\alpha]}$ is the α-root mean value of R^α, $E[\,]$ denotes the expectation operator, α is the Weibull parameter, $\Gamma(.)$ is the Gamma function [11, Eq. 8.310.1], ${}_2F_1(.)$ is the hypergeometric function [11, Eq. 9.14.1], $J_0(.)$ is the Bessel function of the first kind and zeroth order [11, Eq. 8.401], and ω_D is the maximum Doppler shift given in rad/s.

Using the space-time duality of the wireless channel [12], it is readily known that $\omega_D\tau = 2\ d/\ $, where d is the travelled distance, and is the carrier wavelength. Then, the spatial autocorrelation function $A_R(d)$ of R is

$$A_R(d) = \hat{r}^2\,\Gamma^2\left(1+\frac{1}{\alpha}\right)\,{}_2F_1\left(-\frac{1}{\alpha},-\frac{1}{\alpha};1;J_0^2(2\ d/\ )\right) \quad (2)$$

A. The moment-based α-estimator

The moments of the Weibull envelope are given as [10]

$$E[R^k] = \hat{r}^k\Gamma(1+k/\alpha) \quad (3)$$

From (3), it follows that

$$\frac{E^i[R^j]}{E^j[R^i]} = \frac{\Gamma^i\,(1+j/\alpha)}{\Gamma^j\,(1+i/\alpha)} \quad (4)$$

For a particular case in which $i = 2$ and $j = 1$, (4) yields

$$\frac{E^2[R]}{E[R^2]} = \frac{\Gamma^2(1+1/\alpha)}{\Gamma(1+2/\alpha)} \quad (5)$$

Note that the estimator presented in (5) is given in terms of the ratio of the squared first and second moments. Of course, from (4) there are other moment-based estimators, however, the one presented in (5) is given by the lowest integer order.

Given a set of measured data for the fading envelope R, the practical procedure in order to determine the distribution parameter α is to find the root of the transcendental equation (5). In fact, this method provides a simple and low-complexity parameter estimator.

III. The Envelope Power Spectrum

The power spectrum $S_R(\ )$ of the Weibull fading envelope R is the Fourier transform[1] of its autocorrelation function $A_R(d)$ given by (1). Although this leads to an exact calculation, it seems that no closed-form expression can be found. In this section, an *accurate closed-form approximation* to $S_R(\ )$ is derived. To this end, the following expansion of the hypergeometric function ${}_2F_1(.)$ is used [12]

$${}_2F_1\left(-\frac{1}{\alpha}, -\frac{1}{\alpha}; 1; J_0^2(2\ d/\ )\right) = 1 + \frac{1}{\alpha^2}J_0^2(2\ d/\ ) + \frac{1-\frac{1}{\alpha}^{\ 2}}{4\alpha^2}J_0^4(2\ d/\ ) + \frac{1-\frac{1}{\alpha}^{\ 2}\ 2-\frac{1}{\alpha}^{\ 2}}{36\alpha^2}J_0^6(2\ d/\ ) + ... \quad (6)$$

In (6), dropping the terms beyond the second degree, the exact Weibull autocorrelation function $A_R(d)$ (1) can be approximated by $\tilde{A}_R(d)$ as

$$A_R(d) \approx \tilde{A}_R(d) = \hat{r}^2\Gamma^2\left(1+\frac{1}{\alpha}\right)\left(1+\frac{J_0^2(2\ d/\ )}{\alpha^2}\right) \quad (7)$$

The maximum deviation between the exact (1) and the approximate (7) solutions occurs for $d = 0$. Fig. 1 plots this deviation as a functions of α. Indeed, the deviation is *null* for $\alpha = 1$ and less then 1.8% for $\alpha > 1$. It can be seen that, for $\alpha < 1$, the approximation departs steadily from the exact value as α approaches zero. However, $\alpha < 1$, corresponding to a Nakagami-*m* parameter $m < 0.2$, is rarely found in real situations. Thus, for practical purposes ($\alpha \quad 1$), the proposed approximation is indeed *excellent*.

Now, taking the Fourier transform of (7), an *accurate approximation* to $S_R(\ )$ can be calculated in a closed-form formula as

$$S_R(\ ) \approx \hat{r}^2\Gamma^2\left(1+\frac{1}{\alpha}\right)\left[\delta(\ ) + \frac{}{{}^2\alpha^2}K\left(\sqrt{1-\frac{}{2}}\right)\right] \quad (8)$$

for $|\ | < 2/\ $, where $\delta(.)$ is the Dirac delta function and $K(.)$ is the complete elliptic integral of the first kind [11, Eq. 8.112.1]. As a check for the correctness of these results, we note that, for $\alpha = 2$ (Rayleigh condition), (7) and (8) specialize into [12, Eq. 1.3-16] and [12, Eq. 1.3-27], respectively.

[1]The Fourier transform $\mathcal{F}(\beta)$ of a function $f(x)$ is defined here as $\mathcal{F}(\beta) = \int_{-\infty}^{\infty} f(x)\exp(-j\beta x)dx$.

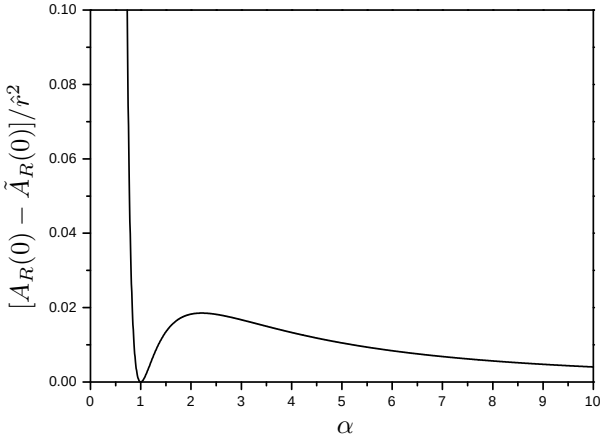

Fig. 1. Deviation of the approximated and exact Weibull autocorrelation functions for $d = 0$

IV. Sample Examples

This section illustrates how the autocorrelation and power spectrum functions of the Weibull envelope vary with different values of the parameter α. Fig. 2 shows, for $\alpha = 0.5, 1, 1.5, 2, ..., 5$, the exact and approximate autocorrelation functions. As already mentioned, for $\alpha = 1$, approximate and exact expressions are coincident. As $\alpha \to \infty$, $A_R(d) \to \hat{r}^2$, i.e., the Weibull process becomes actually a constant function. The approximation (8) to the Weibull envelope power spectrum is compared to the exact formulation (obtained by numerical integration) in Fig. 3. Both exact and approximated spectra are plotted for $\alpha = 0.5, 1$, and 2. (The dc component was omitted in the comparisons.) It can be shown that, for $\alpha > 1$, the differences are seen to be minimal and tend to zero. The counterpart of the unity autocorrelation function as $\alpha \to \infty$ is a purely dc spectrum, i.e., $S_R(\ ) \to \hat{r}^2\delta(\ )$ for $\alpha \to \infty$.

V. Field Trials and Validation

A series of field trials was conducted at the University of Campinas (Unicamp), Brazil, in order to validate the autocorrelation function and the power spectrum of the Weibull envelope. The transmitter was placed on the rooftop of one of the buildings and the receiver travelled through the campus as well as within the buildings. The mobile reception equipment was especially assembled for this purpose. Basically, the setup consisted of a vertically polarized omnidirectional receiving antenna, a low noise amplifier, a spectrum analyzer, data acquisition apparatus, a notebook computer, and a distance transducer for carrying out the signal sampling. The transmission consisted of a CW tone at 1.8 GHz. The spectrum analyzer was set to zero span and centered at the desired

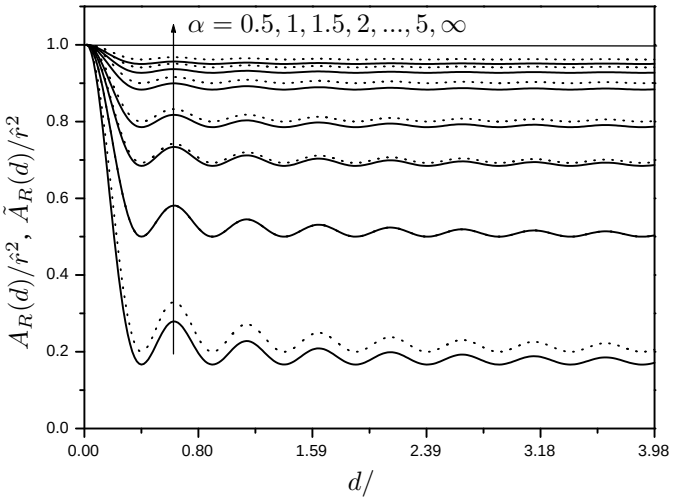

Fig. 2. Weibull autocorrelation function (exact: solid; approximated: dashed)

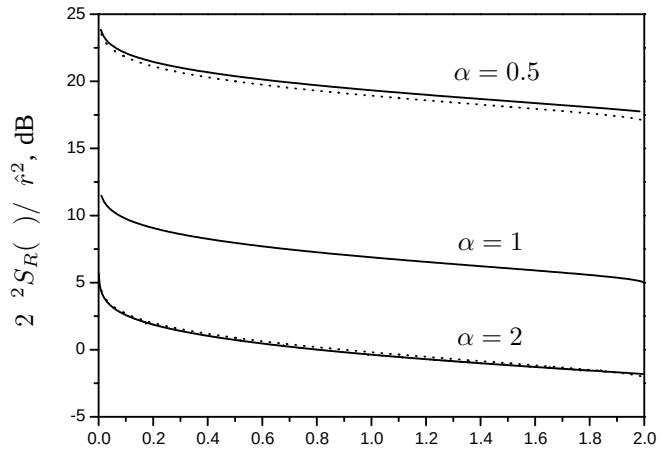

Fig. 3. Weibull envelope power spectrum (exact: solid; approximated: dashed)

frequency, and its video output used as the input of the data acquisition equipment with a sampling rate of $/14$. The local mean was estimated by the moving average method, with the average being conveniently taken over samples symmetrically adjacent to every point. From the data collected, the long term fading was filtered out and the Weibull parameter α, as defined previously, was estimated.

The normalized empirical autocorrelation was computed according to

$$\widehat{A}_R(\Delta) = \frac{\sum_{i=1}^{N} {}^{\Delta} r_i r_{i+\Delta}}{\sum_{i=1}^{N} r_i^2} \tag{9}$$

where r_i is the i-th sample of the amplitude sequence, N is the total number of samples, Δ is the discrete relative distance difference, and $\widehat{A}_R(.)$ denotes an empirical average of $A_R(.)$.

The empirical autocorrelation function was compared against the corresponding theoretical formula (2) and plotted as a function of $d/$ with the same parameter α estimated from the experimental data. Furthermore, a numerical measure of the mean error deviation[2], , was computed for each case. Figs. 4, 5, and 6 show some sample plots comparing the experimental and theoretical autocorrelation data for different values of α. Observe the *excellent* fitting and how the theoretical curve tends to keep track of the changes of concavity of the empirical data. As can be observed, in the three cases the error deviation were smaller than 2%.

In order to check the validity of the Weibull envelope power spectrum formulation (8), we compared it against the measurement data. To this end, we used discrete Fourier transform (DFT)[3] to compute the Fourier transform of the empirical autocorrelation. Thus, the empirical envelope power spectrum S_R was computed. Figs. 7, 8, and 9 show some sample plots comparing the experimental and theoretical power spectrum data for different values of α. Through our measurements, an *excellent* fitting has been observed.

VI. Conclusions

In this paper, we have reported the results of field trials aimed at investigating the second-order statistics of short term fading signals. An *excellent* agreement between the experimental and the theoretical data has been found. The measurements validate the autocorrelation formula derived in an exact manner in [10] for the Weibull fading signal. Moreover, an *accurate closed-form* approximation to the power spectrum of the Weibull envelope was also obtained and validated.

References

[1] H. Suzuki, "A statistical model for urban radio propagation," *IEEE Trans. Commun.*, vol. 25, Jul. 1977.

[2] M. D. Yacoub, "Fading distributions and co-channel interference in wireless systems," *IEEE Antennas and Propagation Magazine*, vol. 42, pp. 150–160, Feb. 2000.

[3] N. H. Shepherd, "Radio wave loss deviation and shadow loss at 900 MHz," *IEEE Trans. Veh. Technol.*, vol. 26, pp. 309–313, Nov. 1977.

[4] H. Hashemi, "The indoor radio propagation channel," *Proc. IEEE*, vol. 81, pp. 943–968, Jul. 1993.

[5] G. Tzeremes and C. G. Christodoulou, "Use of Weibull distribution for describing outdoor multipath fading," in *Proc. IEEE Antennas and Propagation Soc. Int. Symp.*, vol. 1, Jun. 2002, pp. 232–235.

[6] N. S. Adawi, "Coverage prediction for mobile radio systems operating in the 800/900 MHz frequence range," *IEEE Trans. Veh. Technol.*, vol. 37, pp. 3–72, Feb. 1988.

[7] F. Babich and G. Lombardi, "Statistical analysis and characterization of the indoor propagation channel," *IEEE Trans. Commun.*, vol. 48, pp. 455–464, Mar. 2000.

[8] N. C. Sagias, D. A. Zogas, G. K. Karagiannidis, and G. S. Tombras, "Channel capacity and second-order statistics in Weibull fading," *IEEE Commun. Lett.*, vol. 8, pp. 377–379, Jun. 2004.

[9] G. Fraidenraich, M. D. Yacoub, and J. C. S. Santos Filho, "Second-order statistics of maximal-ratio and equal-gain combining in Weibull fading," *IEEE Commun. Lett.*, vol. 9, pp. 499–501, Jun. 2005.

[10] M. D. Yacoub, D. B. da Costa, U. S. Dias, and G. Fraidenraich, "Joint statistics for two correlated Weibull variates," *IEEE Antennas and Wireless Propagation Letters*, vol. 4, pp. 129–132, 2005.

[11] I. S. Gradshteyn and I. M. Ryzhik, *Table of Integrals, Series, and Products*, 6th ed. Academic Press, 2000.

[12] W. C. Jakes, *Microwave Mobile Communications*. New York: Wiley, 1974.

[2]The mean error deviation between the measured data x_i and the theoretical value y_i is defi ned as $\epsilon = \frac{1}{N}\sum_{i=1}^{N}\frac{|y_i - x_i|}{x_i}$, where N is the number of points.

[3]The DFT was implemented by the FFT (Fast Fourier transform) algorithm

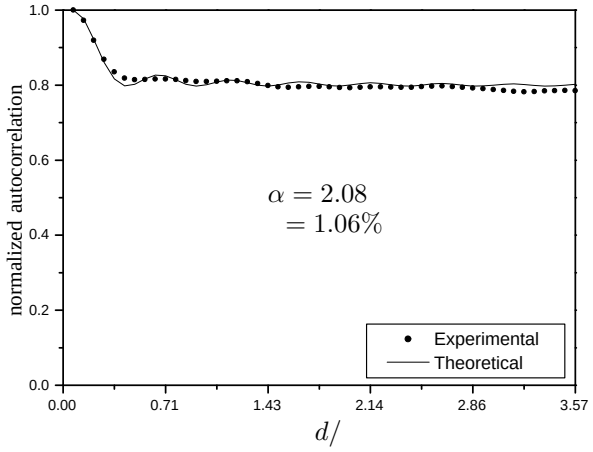

Fig. 4. Empirical versus theoretical autocorrelation function

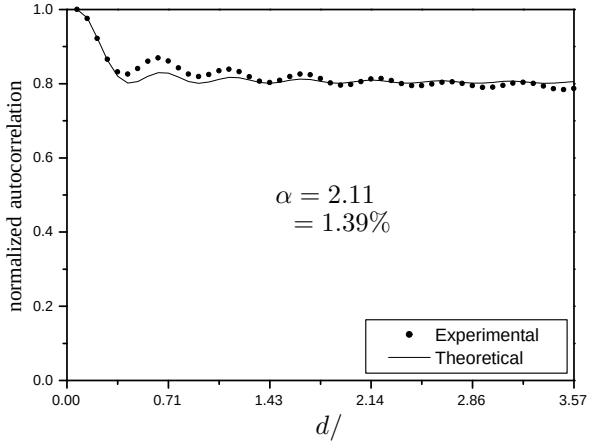

Fig. 5. Empirical versus theoretical autocorrelation function

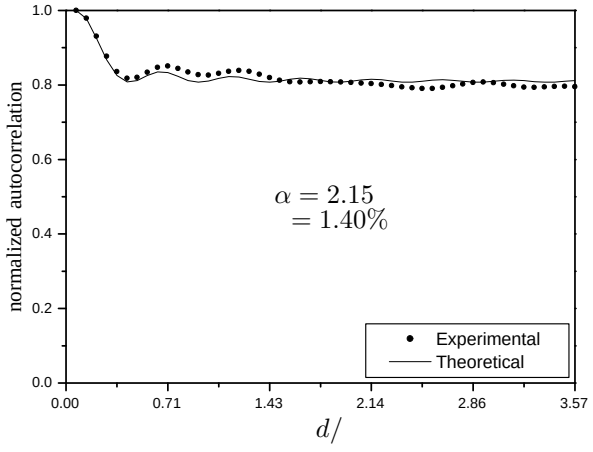

Fig. 6. Empirical versus theoretical autocorrelation function

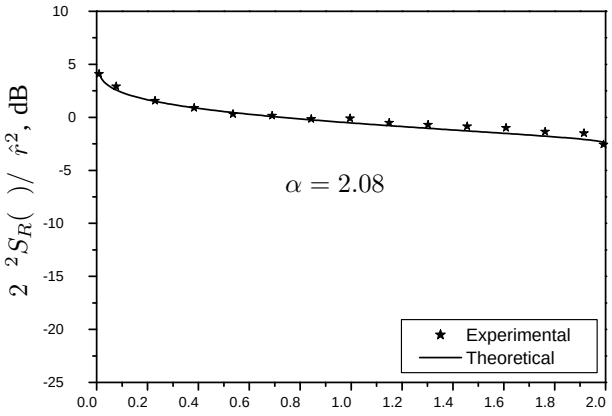

Fig. 7. Empirical versus theoretical envelope power spectrum function

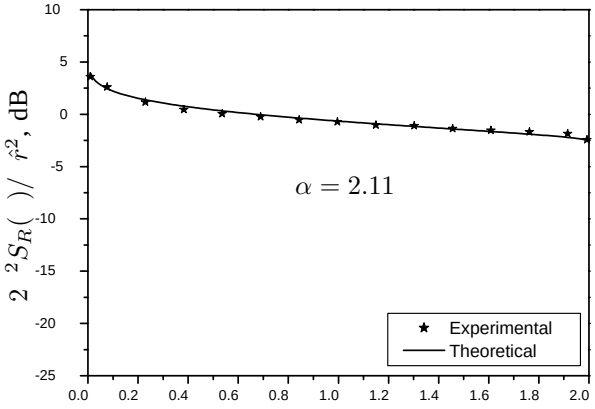

Fig. 8. Empirical versus theoretical envelope power spectrum function

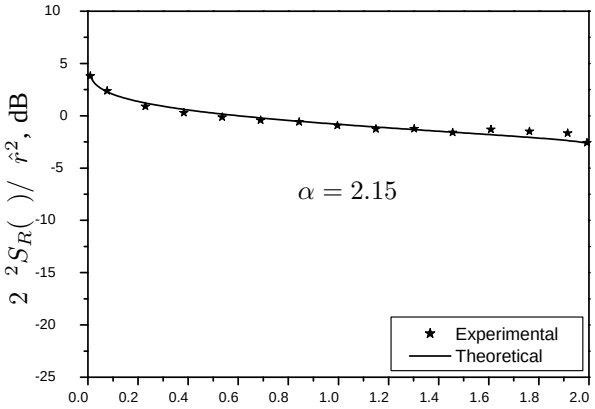

Fig. 9. Empirical versus theoretical envelope power spectrum function